Equation of state of solid ^{4}He

A. Driessen* and E. van der Poll
Natuurkundig Laboratorium, Universiteit van Amsterdam, Valckenierstraat 65, 1018 XE Amsterdam, The Netherlands

Isaac F. Silvera
Lyman Laboratory of Physics, Harvard University, Cambridge, Massachusetts 02138
(Received 15 August 1985)

Isochores of condensed helium have been measured between 0.1 and 2 kbar from $T=2$ K up to the liquid phase. With the results of these measurements and the equation-of-state (EOS) data in the literature the $T=0$ K isotherm was determined up to 6 cm^3/mole. With use of the Mie-Grüneisen model for the thermal properties of the solid- and melting-line data from the literature, a complete EOS for condensed helium including the liquid along the melting line in the density range from 21–6 cm^3/mole was developed. A tentative EOS, mainly based on extrapolations and calculations, is given up to 2.5 cm^3/mole. The results are presented in extensive tables and compared with nearly all relevant data in the literature. Agreement and consistency is found in most cases within the stated experimental error.

I. INTRODUCTION

Although the helium atom is one of the simplest atoms in the Periodic Table of the Elements, in the condensed phase as a many-body system its equation of state (EOS) is exceptionally rich and complex. At $T=0$ K, in equilibrium with its vapor pressure ($P=0$ bars), helium is the only substance which remains in the liquid state. At a finite temperature the liquid state has a superfluid–normal-fluid phase transition. With a modest pressure of $\approx$25 bars (for ^{4}He) the liquid can be solidified. For $P \leq 1.2$ kbar three structures occur: hexagonal-close-packed (hcp), face-centered-cubic (fcc), or body-centered-cubic (bcc) solid structures (see Fig. 1); at higher pressure there is experimental evidence of a new phase.[1]

In this article we present our own new measurements of the isochores at low pressure and include all literature data up to the recent high-pressure shock experiments of Nellis *et al.*[2] The EOS of the solid including pressure, temperature, bulk modulus, and thermal expansion is tabulated for a dense set of molar volumes in the range of 21–6 cm^3/mole ($\approx$25–25 000 bars), with an extrapolation to 2.5 cm^3/mole ($\approx$570 kbar). Extensive use is made of the Mie-Grüneisen model to interpolate and extrapolate the experimental data. The EOS is fitted to a Birch equation to provide P versus V at $T=0$ K.

Helium is an unusual substance in that at low pressure the zero-point energy is larger than the potential energy in the free-energy expression. As a consequence, it is highly compressible and our results cover a density variation of $\approx$8.5 in the solid state. We were unable to find a single set of coefficients from the Birch relation to span this entire range and present two sets, for low and high pressures, to give optimum accuracy.

Several attempts have been made to collect the available data to give a consistent overall picture of the EOS of ^{4}He (see, e.g., Spain and Segal[3]). In the past few years we have made extensive studies of the EOS of the hydrogen isotopes[4,5] and gained considerable experience in correlating and fitting data from a number of thermodynamic measurements. After measuring the isochores of ^{4}He we noted a number of large systematic errors in the EOS treatment of Spain and Segal[3] and decided to reanalyze the entire set of data in the literature to provide a more accurate EOS. As can be expected, the experimental data for ^{3}He are less extensive. An analysis of these data and a resulting tabulation of the EOS of solid ^{3}He is available on request.[5(b)]

This paper is organized as follows: In Sec. II we review the data in the literature; our own experiment and data are described in Sec. III. In Sec. IV we generate the EOS, which is discussed in Sec. V. The extensive table of the EOS is given in an appendix.

II. REVIEW OF EXPERIMENTAL DATA

In this short review we restrict ourselves to the data which are used for generating an EOS or which are compared with our results. In Fig. 1 we show the phase diagram on a log-log scale in the P-T plane. Below 100 kbar one can distinguish three solid phases: a hcp phase below about 15 K, a fcc phase above 15 K and density greater than 12 cm^3/mole, and a small bcc pocket along the melting line at about 1.5 K. At pressures of order 100 kbar, near the melting line, Loubeyre *et al.*[1] have found evidence of a phase transition, while Lévesque *et al.*[6] have suggested that a premelting bcc phase appears, based on a constant-pressure molecular-dynamics calculation. We do not include volume effects of these phase transitions in our EOS. For the hcp→bcc transition[7–14] the grid of the tabulation of our EOS in the Appendix is too coarse, and we refer to the original work given below. The relative volume change for the hcp→fcc transition[11–24] is less than 0.05%, which is much smaller than the error in any absolute experimental volume determination and can be neglected. For the volume change of the fcc→bcc transi-

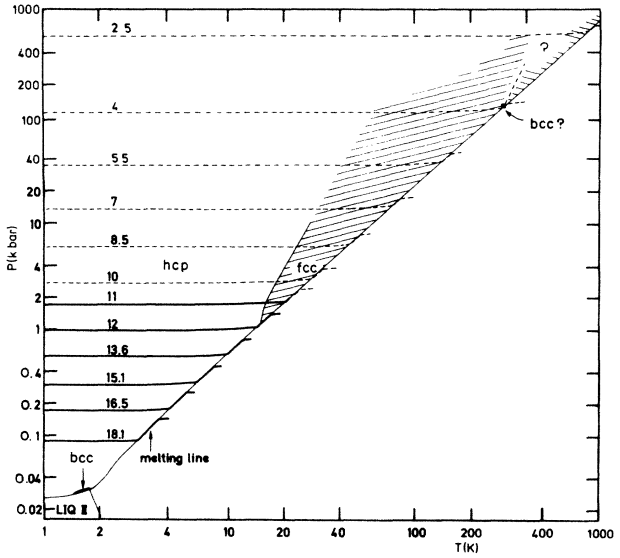

FIG. 1. Phase diagram of ^{4}He on a logarithmic P-T plot. Several isochores are also drawn: solid lines, our experiment; dashed lines, calculated from our EOS. The numbers labeling each curve are the molar volumes (cm^3/mole). The high-pressure phase transition has only been observed at the melting line, and the further behavior is unexplored.

tion[6] there are no experimental data or available estimates from theory.

Stewart[25,26] measured the change in molar volume along an isotherm at $T=4.2$ K between 2 and 20 kbar in two different experiments. Dugdale and Simon[15] made extensive measurements of the molar volume and specific heat up to 3 kbar (including the melting line). They were the first to report the transition between the hcp and fcc phases. Mills and Grilly made measurements of the melting line[27] and later precisely determined the molar volume and other thermodynamic properties[28] along the melting line up to 3.5 kbar. Due to experimental techniques these measurements are restricted to temperatures where cryogenic fluids (He, H_2, or Ne) are available. Therefore an important region ($4.7<T<14.7$ K or $175<P<1100$ bars) is missing. Dugdale and Franck[29] performed specific-heat measurements up to about 1 kbar; for the determination of the molar volume they used the data of Grilly and Mills.[28]

With the specific-heat data[15] one can determine the thermal pressure, and relate the pressure P_0 at $T=0$ K with the melting pressure P_{ms}. With the known volume at the melting line,[28] it is possible to calculate the $T=0$ K isotherm up to 3 kbar and extend this to 20 kbar with the compressibility data of Stewart.[25,26] In this way Spain and Segall[3] were able to present a complete tabulation of the EOS up to 20 kbar.

In several papers Ahlers,[9,30,31] as well as Edwards and Pandorf,[10,32] reported extensive heat-capacity measurements. Jarvis *et al.*[12] measured $\partial P/\partial T$ at low pressure up to 100 bars. Fluid properties have been compiled by Glassford and Smith[33] and by Betts.[34]

Krause and Swenson[35] published a more precise melting line at moderate pressures and Mills *et al.*[36] provided an extension up to 20 kbar. These authors also give an EOS of the liquid, starting from the melting line, for pressures up to 20 kbar. The data are based on relative volume measurements with a piston technique. Loubeyre *et al.*[1] measured the melting line in a diamond-anvil cell up to 360 K and 160 kbar.

Young *et al.*[37] used a semiempirical "exponential-six" interatomic pair potential for calculating the EOS up to 120 kbar, which compares reasonably well with experimental data below 20 kbar (Ref. 36) and the room-temperature melting point (Ref. 1). At even higher pressures (120 kbar $<P<$ 250 Mbar) they used a linear-muffin-tin-orbitals (LMTO) electron-band—theory calculation. Very recently, Nellis *et al.*[2] performed shock-compression experiments on liquid helium with a maximum final pressure of 560 kbar, which allows a qualitative check on the reliability of the calculations of Young *et al.*[37]

The hcp-to-fcc transition detected with specific-heat measurements[15] has been the subject of a theoretical study by Holian *et al.*[23] and Young and Alder,[24] and has been followed up to 9 kbar by optical[22] and calorimetric methods.[20]

The existence of a γ phase (bcc) was first observed by Vignos and Fairbank[7] in sound-velocity measurements. Grilly and Mills,[8] Ahlers,[9] Edwards and Pandorf,[10] Jarvis *et al.*,[12] Grilly,[13] and Hoffer *et al.*[14] determined the thermodynamic properties at low temperature below 2 K including the γ phase. In the superfluid phase Maynard has presented EOS tables for $T\simeq 1$ K up to 25 bars, while Landau and Ihas have measured isochores and present EOS tables from 25 bars up to the melting line.[38]

III. MEASUREMENT OF ^{4}He ISOCHORES

When we started to make isochoric pressure measurements on H_2 and D_2 several years ago, a few isochores of ^{4}He were measured for comparison with literature values as a control on the measurement technique. Substantial deviations from values in the tabulation of Spain and Segall[3] were found. Therefore we decided to measure a dense set of isochores from 50 bars to 2 kbar from $T\approx 1$ K up to the liquid phase.

The experimental equipment, which has been used earlier for measurements on H_2 and D_2 is described in detail in Refs. 40 and 5(b). The measuring technique consisted of confining helium in a high-pressure cell of fixed volume and of measuring the pressure variation as a function of temperature. We used a cylindrical vessel made from BeCu 25 with a volume of 1.2 cm^3 and a maximum working pressure of 2 kbar, shown in Fig. 2. Pressure was detected with resistance-strain gauges (BLH Electronics, Inc, Model no. FSM 25-35-59), which were attached at the thin part of the walls and on a strain-free bar in good thermal contact with the cell for temperature compensation (see Fig. 3). The strain-gauge pressure transducers were calibrated at room and cryogenic temperatures at the Van der Waals Laboratorium of the University of Am-

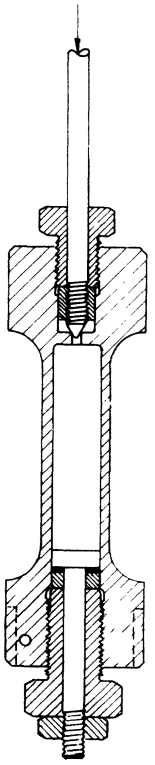

FIG. 2. Beryllium copper isochore cell.

sterdam, with an absolute accuracy of 2 bars.

For temperature control between 1.1 K and room temperature, the cell was mounted inside two concentric brass cans, which could be separately evacuated or filled with gas for thermal heat exchange. The outer can was immersed in liquid helium (see Fig. 3). Below 100 K the temperature could be stabilized within 0.05 K and measured with a calibrated germanium thermometer within 0.1 K. The cell was connected to a high-pressure helium-gas-generating system ($P < 7$ kbar) with a thin capillary (inner diameter of 0.16 mm), which could be closed by a valve at the top of the cryostat. During measurements the capillary was frozen directly above the brass cans by introducing exchange gas into the capillary vacuum tube. In this way the amount of helium sample could be kept constant within 0.01 mol %.

For a measurement run we normally selected a P,T point in the fluid phase by applying this pressure to the cell held at the desired temperature. Once this condition was reached, the high-pressure valve at the cryostat was closed and heating of the capillary was stopped. Temperature was changed in small steps and pressure was registered after allowing for thermal equilibrium. Pressure readings could be reproduced within calibration accuracy in going up and down in temperature on an isochore. The number of points measured on an isochore varied up to more than 100. In all we studied 30 helium samples with different densities.

As an example, we show in Figs. 4–6 three isochores with our data points after correction for the small expan-

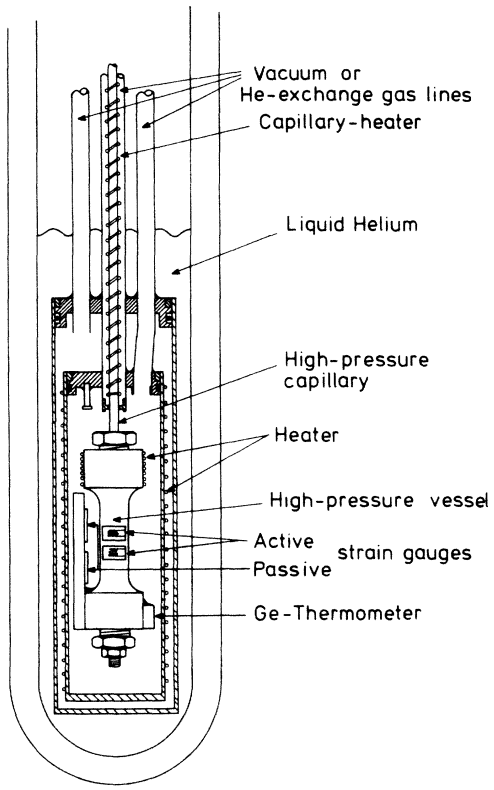

FIG. 3. Isochore cell mounted in the cryogenic environment.

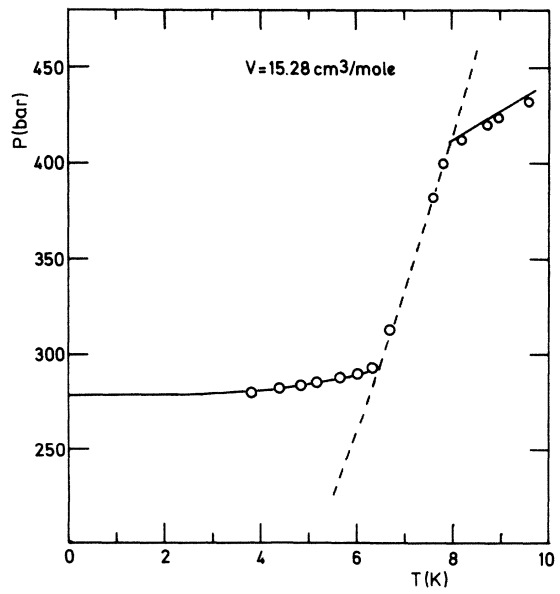

FIG. 4. Experimental isochore at 15.28 cm^3/mole. Open circles, experimental points; solid line, calculated from our EOS as given in the Appendix; dashed line, melting line.

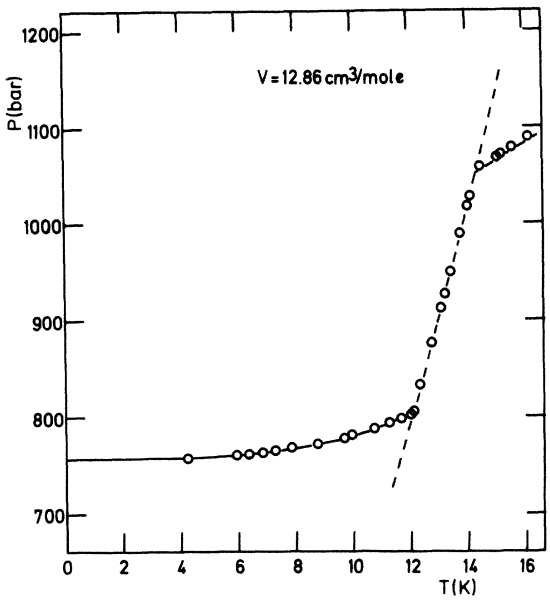

FIG. 5. Experimental isochore at 12.86 cm^3/mole. Open circles, experimental points; solid line, calculated from our EOS as given in the Appendix; dashed line, melting line.

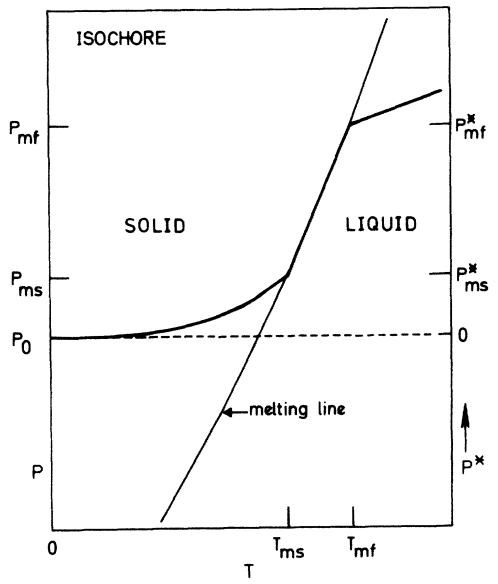

FIG. 7. Schematic isochore.

sion of the pressure vessel due to pressure changes, together with a calculation based on the Mie-Grüneisen model for the solid as presented in the following section. As can be seen, the calculation fits the data within the experimental scatter.

A convenient way of displaying the results of the 30 different experimental runs is to give the thermal pressure at the melting line in the solid, P^*_{ms}, and in the fluid, P^*_{mf} [see Eqs. (1) and (2) for definitions], as a function of P_0, the pressure at $T=0$ K, with all pressures taken on an isochore (see Fig. 7). Figure 8 shows P^*_{ms} as a function of P_0. Our isochores are given by squares. The values of Spain and Segall (triangles) with a stated error of 5% in P^* are in fairly good agreement with our data, which have nearly the same accuracy. The solid line is taken from our EOS as tabulated in the Appendix, which comes out as a smooth fit through the different data points. This line is a result of the averaging of our data and specific-heat data from different authors, as will be discussed in the following section.

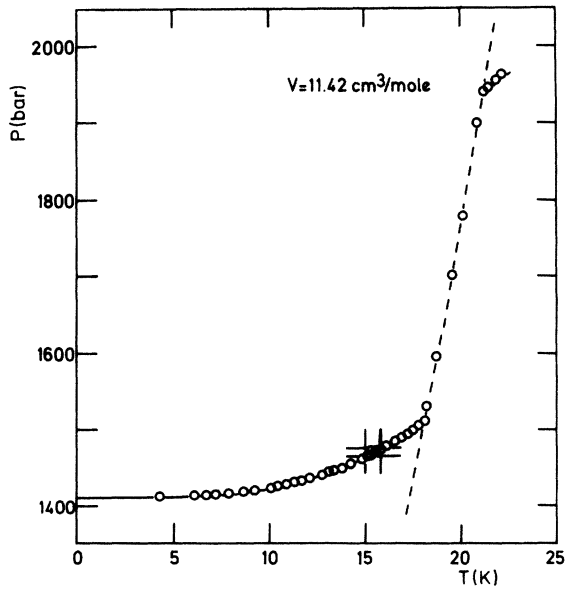

FIG. 6. Experimental isochore at 11.42 cm^3/mole. Open circles, experimental points; solid line, calculated from our EOS as given in the Appendix; dashed line, melting line. The small rectangle at 15 K is amplified in Fig. 10 to show the hcp→fcc transition in detail.

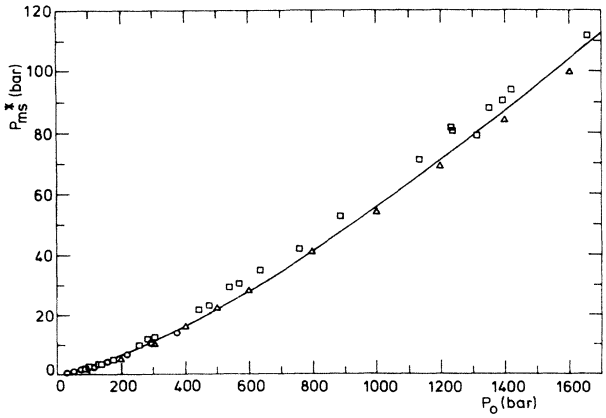

FIG. 8. Thermal pressure P^*_{ms} in the solid along the melting line as a function of pressure P_0 at $T=0$ K. Squares, our experimental isochores; triangles, Spain and Segall (Ref. 3); circles, Ahlers (Ref. 31); solid line, from our EOS.

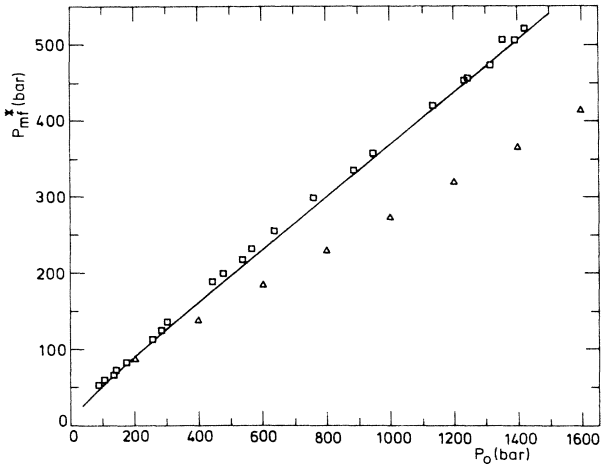

FIG. 9. Thermal pressure P^*_{mf} in the fluid along the melting line as a function of pressure P_0 at $T=0$ K. Squares, our experimental isochores; triangles, Spain and Segall (Ref. 3); solid line, from our EOS.

Figure 9 is a similar display of P^*_{mf} as a function of P_0. Our data (squares) and the EOS (solid line) can only be compared with the prediction of Spain and Segall (triangles). As can be seen, there is a severe disagreement well outside the stated errors. This will be discussed in Sec. V.

Our isochores also crossed the fcc→hcp phase-transition line. Figure 10 shows in detail the pressure change due to this transition at $V=11.42$ cm^3/mole. In the determination of the EOS we neglect this pressure step, as our error in the determination of P^* is of the same order of magnitude.

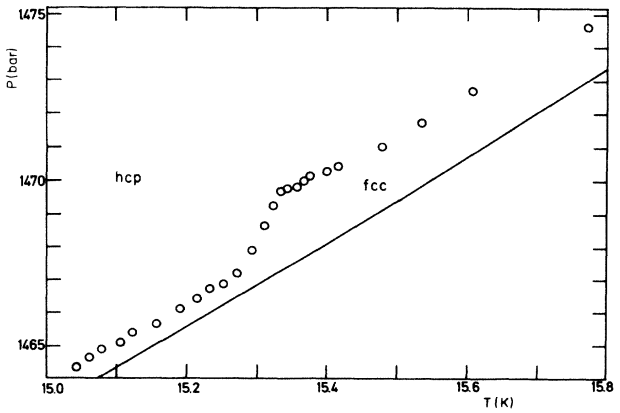

FIG. 10. Enlarged section of our experimental isochore at 11.42 cm^3/mole shown in Fig. 6. Open circles, experimental points; solid line, calculated from our EOS.

IV. GENERATION OF THE EOS

A. The $T=0$ K isotherm

Reviewing the literature, one finds only very few direct experimental determinations of the molar volume. In 1953 Dugdale and Simon[15] measured the molar volume V_{mf} and the volume change ΔV_m along the melting line. They gave a table of smooth values between 4 and 26 K, but no estimate of the accuracy. Later Grilly and Mills[28] repeated these measurements, apparently with greater accuracy, in the temperature range where cryogenic fluids were available, i.e., $1.3<T<4.7$ K (helium) and $14.7<T<30.8$ K (hydrogen and neon). Their molar volume determination in the fluid along the melting line (stated accuracy 0.1%) is in agreement within 1% in the region of overlap with Dugdale and Simon.[15]

Grilly[13] studied in detail the PVT relation between 0.3 and 2 K. His volume data, which are based on the V_{mf} of Grilly and Mills[28] at 1.3 K, are in excellent agreement (within 0.05%) with the direct measurements of Edeskuty and Sherman,[41] and 0.5% lower than those of Keesom and Keesom.[42] As a conclusion, the V_{mf} data of Grilly and Mills[28] seems to be reliable with an estimated error of a few tenths of a percent at low pressures and less than 1% at the highest pressure (3.5 kbar).

Besides this class of measurements, there are two sets of 4.2-K compressibility data by Stewart[25,26] using the piston technique. The pressure of his reference volume was set to 2 kbar because of the large starting compressibility of helium at low pressures and friction of his apparatus. His first data points were at 3 kbar.

The problem in establishing the $T=0$ K isotherm consists of connecting the volume data along the melting line at relatively low pressure with the compressibility data at essentially $T=0$ K at higher pressure, with only a small region of overlap in pressure. In order to make use of the total set of experimental isochoric data in the literature along with our own data, we separate the temperature-dependent part of the pressure from the total pressure [also see Eqs. (6) and (10)],

$$P_{ms}(V,T)=P_0(V)+P^*_{ms}(V,T) \tag{1}$$

and

$$P_{mf}(V,T)=P_0(V)+P^*_{mf}(V,T)\ . \tag{2}$$

For P^*_{ms} and P^*_{mf} we use empirical expressions

$$P^*_{ms}(V,T)=C_0+C_1P_0(V)/100+C_2[P_0(V)/100]^2 \tag{3}$$

and

$$P^*_{mf}(V)-P^*_{ms}(V)=C'_0+C'_1P_{ms}(V)+C'_2[P_{ms}(V)]^2+C'_3[P_{ms}(V)]^3\ . \tag{4}$$

The coefficients are determined by making a weighted least-squares fit to the experimental data. For Eq. (3) we needed two different sets of coefficients for $P<400$ bars and $P>400$ bars. For the low-pressure fit we use the following data points: ten points from specific-heat data of Ahlers,[31] eight points of Edwards and Pandorf,[32] and seven points from $\partial P/\partial T$ measurements of Jarvis *et al.*[12]

For the higher pressure we take 15 data points of our own, three from Ahlers,[31] six from Dugdale and Franck,[29] and ten from the tabulation of Spain and Segall.[3] The resulting coefficients are given in Table I. For the determination of the coefficients of Eq. (4), only our experimental data are available. Table I (third column) gives the result of our fit of 22 data points.

With the direct-volume measurements in the literature and the analytical functions (3) and (4), we are able to generate the $T=0$ K isotherm. Like Stewart,[25,26] who fitted his experimental data points with a modified Birch relation, we start with

$$P=P_0+\tfrac{3}{2}K_0Y^5(Z+CZ^2+DZ^3)\ . \tag{5}$$

P_0 is the pressure and K_0 the bulk modulus at $V=V_0$; $Y=(V_0/V)^{1/3}$ and $Z=Y^2-1$; C and D are coefficients to be determined from experiment. (In the case of Stewart the cubic term DZ^3 was omitted.) We determine the coefficients of this relation by a weighted least-squares fit of $P(V)$, where we minimize relative volume deviations

$$[V_{\rm expt}(P)-V_{\rm calc}(P)]/V_{\rm expt}(V)\ .$$

The weight is determined by the experimental accuracy of $V_{\rm expt}(P)$; $V_{\rm calc}(V)$ is calculated with the aid of Eq. (5).

We were unable to find one set of coefficients for the Birch relation, Eq. (5), which can represent all experimental data without serious systematic deviations. We therefore split the fit into a high-pressure and low-pressure part. This difficulty is not astonishing, as the low-pressure part of the $T=0$ K isotherm of helium is highly determined by the zero-point motion and the Birch equation is not specifically developed to account for this behavior.

For the low-pressure isotherm, 21–10 cm^3/mole, we use several sets of experimental data for our least-squares fit. The most accurate direct-volume determinations are the measurements of Grilly and Mills[28] in the liquid at the melting line. We use Eqs. (3) and (4) to relate the melting pressure to corresponding $T=0$ K pressure at the same volume. To this set of data we give the highest weight.

Grilly and Mills[28] also measured the volume change at the melting line due to freezing to determine $V_{ms}(P_{ms})$ with a slightly smaller accuracy than the liquid volumes. The volumes V_{ms} we relate to the volumes at $T=0$ K with aid of Eq. (3). Similarly, we use $V_{ms}(P)$ data of Grilly.[13] Because of the irregularities introduced by the low-pressure bcc phase along the melting line, we omit this temperature and pressure region in our fit.

Dugdale and Simon[15] give a set of smooth $V_{mf}(T_m)$ data in the range 18–10 cm^3/mole, which we believe are less accurate than those of Grilly and Mills,[28] but with the advantage of no gap in temperature. From these data we find, with the aid of Eqs. (3) and (4), additional points on the isotherm at $T=0$ K, which we give the lowest weight. The resulting coefficients for the Birch relation (5), obtained with the least-squares fit, are given in Table II.

At higher density, above 2 kbar, there are two compressibility runs of Stewart.[25,26] With the aid of the low-pressure isotherm just determined, we can redetermine his reference volume to be 10.688 cm^3/mole instead of 10.7 cm^3/mole in his first run[25] and 10.694 cm^3/mole instead of 10.72 cm^3/mole in his second run.[26] In this way we get 12 points from his 1963 run, which we give a high weight in our fit, and eight points from his 1956 run with a lower weight. We also include data points already used in the low-pressure fit with molar volume smaller than 11.2 cm^3/mole. Above 20 kbar there are no available static experimental volume data at $T=0$ K. Young *et al.*[37] give, however, a calculation of the EOS at very high pressure. At moderate high pressure they use a semiempirical "exponential-six" potential, whose parameters are fitted to the experimental solid and liquid data up to 20 kbar (Ref. 36) and to the melting data (Ref. 1) up to 120 kbar. At higher pressure they use the LMTO method to calculate the pressure and total energy of zero-temperature helium up to 250 Mbar. They choose their potential in such a way that they can match the $T=0$ K static lattice pressure predicted by the "exponential-six" potential. If one compares the predicted single- and double-shock Hugoniot data calculated with the LMTO potential with recent

TABLE I. Coefficients for the empirical expressions (3) and (4) for the thermal pressure at the melting line.

	Eq. (3)		Eq. (4)
Coefficients	Low pressure	High pressure	
C_0 (bar)	−0.269 282	−3.5743	17.6614
C_1	2.355	4.5968	0.369 03
C_2 (bar^{-1})	0.393 365	0.146 84	$-0.132\,13\times10^{-3}$
C_3 (bar^{-2})			$0.450\,667\times10^{-7}$

TABLE II. Coefficients for the Birch relation (5) for the low- and high-pressure regions. It is recommended that one switch from one coefficient to the other at 10.5 cm^3/mole.

	Low pressure	High pressure
P_0 (bar)	124.8176	−355.0552
V_0 (cm^3/mole)	17.2915	18.7141
K_0 (bar)	852.0341	819.5402
C	1.184 277	1.419 006
D	2.084 812	0.089 231
Region of validity for V (cm^3/mole)	9.2–21	≤10.9
Region of validity for P (kbar)	0.025–4.3	≥1.8

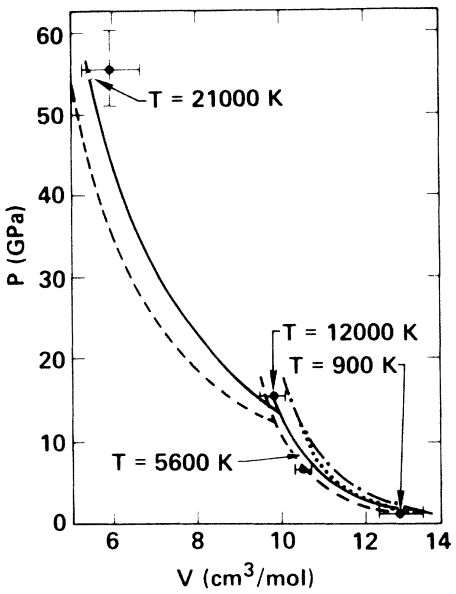

FIG. 11. Comparison of experimental and theoretical helium Hugoniot curves. Points with error bars, experiment by Nellis *et al.* (Ref. 2); dashed line, LMTO calculation by Young *et al.* (Ref. 37); for other curves, see Ref. 2.

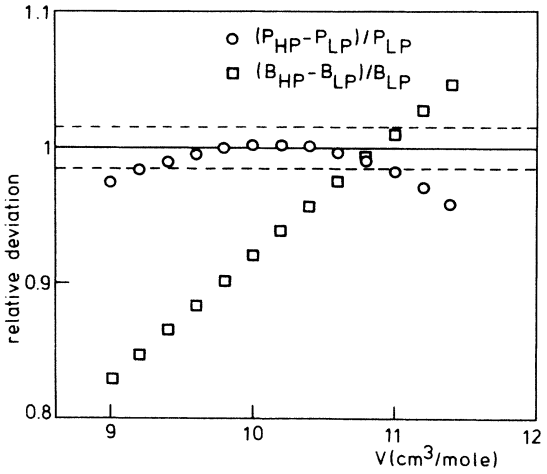

FIG. 12. Relative deviation of high-pressure isotherm values from the low-pressure isotherm values in the region of overlap. Circles, pressure values; squares, values for the bulk modulus; dashed line, error for the pressure in the low-pressure isotherm corresponding to ±0.3% uncertainty in the molar volume.

experimental data by Nellis *et al.*,[2] one finds reasonable agreement (see Fig. 11 taken from Ref. 2). Nellis *et al.* give a single-shock point at 156 kbar, $V=9.78\pm0.30$ cm^3/mole. The LMTO calculations of Young *et al.* give 9.8 cm^3/mole. For the double-shock point Nellis *et al.* give 558±47 kbar, $V=5.87\pm0.71$ cm^3/mole, where Young *et al.* give 4.9 cm^3/mole, which is comparable but clearly outside the experimental error bars.

Altogether we find it worthwhile to include six P,V points at $T=0$ K from the LMTO calculation of Young *et al.* in the range 100—1500 kbar in the fit for the Birch relation (5), bearing in mind that the error will increase quickly with pressure. From a least-squares fit to all high-pressure data points, we get new coefficients for the Birch relation, which are given in Table II.

Figure 12 compares the low-pressure (LP) and high-pressure (HP) isotherms in the region of overlap: 9—11.4 cm^3/mole corresponding with 5—1.5 kbar. Plotted are $(P_{HP}-P_{LP})/P_{LP}$ and $(B_{HP}-B_{LP})/B_{LP}$ (P is the pressure and $B=-V\partial P/\partial V$ the bulk modulus). There is a large region of overlap in pressure within the experimental uncertainty of ±0.3% in molar volume (dashed line in Fig. 12). If we also consider the first derivative, the bulk modulus, the optimum volume to switch from the LP to the HP isotherm is 10.5 cm^3/mole. The tabulation of the EOS in the Appendix is done in this way.

B. The EOS at $T\neq0$ K

Once we have an analytical expression for the $T=0$ K isotherm, we can study the influence of temperature on the EOS. Similar to the work of Spain and Segall,[3] we make use of the Mie-Grüneisen picture for the solid (see also Refs. 4 and 5). One starts with the Helmholtz free energy, which can be separated into a zero-temperature part F_0 and an incremental thermal part F^*,

$$F(V,T)=F_0(V)+F^*(V,T)\ . \tag{6}$$

The pressure P, the bulk modulus B, and the thermal-expansion coefficient α are determined from the thermodynamic relations

$$P=-\left[\frac{\partial F}{\partial V}\right]_T, \tag{7}$$

$$B=-V\left[\frac{\partial P}{\partial V}\right]_T, \tag{8}$$

$$\alpha=\left[\frac{1}{V}\right]\left[\frac{\partial V}{\partial T}\right]_P=-\frac{1}{B}\left[\frac{\partial P}{\partial T}\right]_V, \tag{9}$$

and with Eq. (6) one gets

$$P(V,T)=P_0(V)+P^*(V,T)\ , \tag{10}$$

$$B(V,T)=B_0(V)+B^*(V,T)\ , \tag{11}$$

and as $\partial P_0/\partial T$ is zero by definition,

$$\alpha=\alpha^*(V,T)\ . \tag{12}$$

Assuming the lattice vibrations to be responsible for the thermal pressure and neglecting other terms, one can write within the Debye approximation

$$P^*(V,T)=[\gamma(V)/V]U^*(V,T)\ , \tag{13}$$

where U^* is the temperature-dependent part of the internal energy, and

$$\gamma(V)=-\frac{d\ln\Theta_D(V)}{d\ln V}\ , \tag{14}$$

with Θ_D the Debye temperature. Evaluating the internal energy term U^* in terms of the Debye function, one gets

$$P^*(V,T)=\frac{9\gamma(V)RT^4}{V\Theta_D^3}\int_0^{x_D}\frac{x^3}{e^x-1}dx\ , \tag{15}$$

where R is the gas constant and $x_D=\Theta_D/T$.

As can be seen, the only independent parameter to be determined is $\Theta_D(V)$. We make the following ansatz, already used for hydrogen in Ref. 4:

$$\Theta_D(V)=\exp\left[\sum_k c_k x^k\right]\ , \tag{16}$$

where $x=\ln(V/V_0)$. This form is inspired by the expression

$$\ln(\omega/\omega_0)=\beta-\gamma\ln(V/V_0)$$

used successfully by Berkhout and Silvera[4] to fit the density dependence of phonon frequencies ω in solid H_2. In order to determine the coefficients for Eq. (16), we make a weighted least-squares fit of the thermal pressure at the melting line $P^*_{ms}(T_{ms},V)$ using Eq. (15), which contains $\gamma(V)$ and $\Theta_D(V)$ both explicitly and in the upper limit of the integral. As data input we use 16 $P^*(T_{ms},V)$ points equally spread in molar volume from 20.8 to 6.4 cm^3/mole. From relation (3) with the low-pressure coefficients, we take seven points and five points with the high-pressure coefficients. At molar volumes smaller than 9.5 cm^3/mole, there are no available experimental data for P^*. Dugdale,[43] however, describes a method to obtain $P^*(V)$ at higher density with the aid of an equation similar to (15). He uses an extrapolation of $\Theta_D(V)$ based on the assumption

$$\Theta_D(V)=C\frac{\partial^2U(V)}{\partial R^2}\ , \tag{17}$$

where $U(V)$ is the internal energy and $R=\text{const}\times V^{1/3}$ is the interatomic distance, $\partial^2U/\partial R^2$ is evaluated from the $T=0$ K isotherm, and the proportionality constant C is determined at low density by comparing with the heat capacity measurements by Dugdale and Simon.[15] The resulting P^* is in essential agreement with our own experimental results.

Spain and Segall[3] have followed the same method and get a $\Theta_D(V)$ and $\gamma(V)$ at high density in good agreement with Dugdale. We did not repeat these calculations; instead we use four values of $P^*(T_{ms},V)$ from the tables of Spain and Segall at high densities. The resulting coefficients of the least-squares fit are given in Table III.

TABLE III. Coefficients for the Debye temperature (in K) in Eq. (16).

V_0 (cm^3/mole)	21.913 43
C_0	3.008 66
C_1	−2.603 477
C_2	−0.371 863
C_3	−0.034 688

C. The molar volume of the liquid along the melting line

Our isochoric measurements, which extend up to the liquid phase along the melting line, together with the molar volume data in the literature, enable us to include volume data of the liquid in our tabulation of the EOS in the Appendix. For this we need an analytical expression for the fluid volume at the melting line V_{mf}. We assume the following empirical relation for the volume change on an isobar (see Fig. 13):

$$\left[\frac{V_{mf}-V_0}{V_0}\right]_P=A+BV_0+CV_0^2+DV_0^3\ , \tag{18}$$

where V_0 is taken from our $T=0$ K isotherm. For the determination of the coefficients we use our own isochoric data. We relate our pressure data at constant volume to volume data at constant pressure by the equations

$$V_f(P_{mf},T_{mf})=V(P_0,T=0)\ \ (V\text{ constant})\ ,$$

$$V_0(P_{mf},T=0)=V(P_{mf},T=0)\ \ (P\text{ constant})\ ,$$

where $V(P,T=0)$ is taken from our $T=0$ K isotherm at pressure P.

Besides these data, which are restricted to pressures below 2 kbar, we use literature data for the volume change on melting. For this we expand Eq. (18):

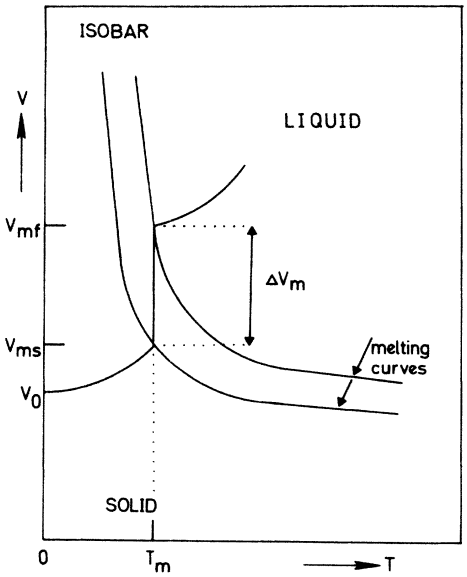

FIG. 13. Schematic isobar.

$$\left[\frac{V_{mf}-V_0}{V_0}\right]_P=\left[\frac{V_{mf}-V_{ms}}{V_0}\right]_P+\left[\frac{V_{ms}-V_0}{V_0}\right]_P . \quad (19)$$

$[(V_{ms}-V_0)/V_0]_P$ can be determined using relation (3) and transforming pressure data and constant volume to volume data at constant pressure as shown above for our own data. For $[(V_{mf}-V_{ms})/V_0]_P$ we use the following literature data:

(i) Grilly and Mills[28] measured very accurate V_{mf} and, with somewhat lower accuracy, V_{ms} between 23 and 10 cm^3/mole, with a gap between 17.6 and 12.7 cm^3/mole.

(ii) Dugdale and Simon[15] did the same for 18—10 cm^3/mole, but with less accuracy.

(iii) Grilly[13] determined the volume change on melting at low density. Because of the irregularities involved with the hcp→bcc transition, we use his data only at densities larger than those of the bcc phase.

(iv) Mills *et al.*[36] measured the volume change with a 10% accuracy at four points between 6.5 and 7.2 cm^3/mole.

(v) Loubeyre *et al.*[1] give an estimate for the volume change on melting in the temperature range 265—280 K: $\Delta V/V=3.1\pm0.04$. Together with an extrapolation of our EOS of the solid, which gives $[(V_{ms}-V_0)/V_0]_P=2.9$ at 4.3 cm^3/mole, we get data for Eq. (19) at very high pressure.

(vi) Young *et al.*[37] give calculated values of the volume change. We use some of these between 5 and 4.3 cm^3/mole as extra data points with a low weight.

A weighted least-squares fit to these data results in the coefficients for Eq. (18), as given in Table IV.

D. The melting line

For the development of the EOS as outlined above, we had to use the melting line, and in the tabulation in the Appendix a dense set of P_{ms}, T_{ms} points will be given explicitly. Several melting-line data are given in the literature, sometimes as an analytical function, sometimes in the form of tables. In order to get an EOS, which reflects as close as possible the full experimental accuracy of the melting line, we start with the Simon melting equation:[44]

$$P_{ms}=C_0+C_1T_{ms}^{C_2} . \quad (20)$$

The coefficients for some temperature regions can be found in the literature, whereas in other regions we determine the coefficients by a weighted least-squares fit.

TABLE IV. Coefficients for the volume change on an isobar, Eq. (18).

A	5.405 38
B (cm^3/mole)$^{-1}$	0.23647
C (cm^3/mole)$^{-2}$	−0.026 584 1
D (cm^3/mole)$^{-3}$	$0.948\,709\times10^{-3}$

1. $1.772<T_m<5$ K

At the lowest temperature, from 0.3 to 2 K, Grilly[13] determined the melting line very accurately. In our EOS we will neglect the bcc phase and the minimum in the melting pressure at 0.775 K; therefore we use his data only above the upper triple point of the bcc→hcp phase transition at 1.772 K. From 1.5 to 4 K there are tabulated data from Swenson[45] which are in reasonable agreement with those of Grilly[13] below 2 K and at 4 K with those of Krause and Swenson.[35] Grilly and Mills[28] also give a melting line in the same region, which shows larger disagreement with Krause and Swenson. We therefore determined the coefficients of the Simon equation (20) in the temperature region from 1.772 to 5 K with a standard error of 1% in pressure with respect to the data of Grilly,[13] Swenson,[45] and Krause and Swenson.[35] The coefficients are given in Table V, first column.

2. $4<T<25$ K

Krause and Swenson[35] measured the melting line within 0.01 K from 4 to 25 K. Their result is in agreement with the data of Mills and Grilly[27] and of Crawford and Daniels.[46] Their coefficients of the Simon equation (20) are given in Table V, second column.

3. $25<T<100$ K

Mills *et al.*[36] measured four melting points from 75.19 to 97.2 K. They determined the coefficients of the Simon equation (20) by a fit through their data points in combination with data of Grilly and Mills[28] and Crawford and Daniels.[46] Their coefficients are given in Table V, third column.

4. $100<T<350$ K

The highest melting temperatures and pressures have been reached in the diamond-anvil cell by Loubeyre *et al.*[1] In Fig. 2 of their paper they show a cusp in the melting line at 300 K, which is interpreted as a fcc→bcc triple point by Lévesque *et al.*[6] In order to get an analytical form up to 350 K, we took the data points tabulated by Loubeyre *et al.*[1] (only three), together with four points from their calculation with a modified Aziz potential with a lower weight. We also took the data points of Mills *et al.*[36] and ended with the coefficients for the Simon equation (20) as given in Table V, fourth column, with a standard deviation in pressure of 0.8%. As pointed out by Loubeyre *et al.*,[1] because of the possible phase transition at 300 K, extrapolation above the highest experimental point at 350 K will probably introduce large errors. Our fit, which follows the experimental points within the stated accuracy in the pressure reading (2%), is not suitable to show the cusp in the melting line. However, the error introduced in this way in our EOS will be small in comparison with other error sources at these high densities.

TABLE V. Coefficients for the Simon melting equation (20).

	I	II	III	IV
C_0 (bar)	−8.052 367	−20.6	−8.112	745.582
C_1 (bar/K)	15.407 93	17.452	16.91	15.5848
C_2	1.580 795	1.546 81	1.555	1.563 955
Region of validity for T (K)	1.772–4.5	4–25	14–100	75–300
Region of validity for P (kbar)	0.03–0.16	0.13–2.5	1–20	14–120
Source	Own fit based on Refs. 33, 36, and 45	Krause and Swenson[a]	Mills *et al.*[b]	Own fit based on Refs. 1 and 34

[a]Reference 33.
[b]Reference 34.

E. Tabulation of the EOS

We now have sufficient data available to give a complete tabulation of the EOS. The Appendix contains two tables (Tables VI and VII). In the first one an EOS from 21 to 6 cm^3/mole is given; in the second one an extrapolation to highest densities of 2.5 cm^3/mole is given. At densities from 21 to 10.5 cm^3/mole we use our low-pressure $T=0$ K isotherm; thereafter we switch to our high-pressure isotherm. For the melting line we make use of four sets of coefficients for Eq. (20), as explained in the preceding subsection. At low temperature we start with the first set and at 4.5 K switch over to the second one (Krause and Swenson[35]). At densities higher than 10.5 cm^3/mole we use the third set (Mills *et al.*[36]) and above 100 K the fourth. For all pressure ranges we calculate the thermal pressure in the solid with the same $\Theta_D(V)$, Eq. (16), with the coefficients of Table III. In spite of the lack of any direct experimental data, with the exception of the recent shock-wave data, we include a rather tentative EOS at very high density up to 2.5 cm^3/mole, which is basically a extrapolation of our analytical functions used in the high-pressure EOS.

From the comparison of our total EOS with the experimental data as given below in the discussion, we can estimate the maximum error in molar volume being about 0.5% for the low-pressure EOS up to densities of 10.5 cm^3/mole. At higher densities, from 10.5 to 6 cm^3/mole, the error will be 0.5% to 1.5%. For the extrapolated EOS we estimate the maximum error to be 2.5% to 20% in molar volume.

V. DISCUSSION

In the preceding sections we developed an EOS for ^{4}He. We used results from the literature, our own measurements, and the Mie-Grüneisen model. It is important to know how all the different data compare to each other, i.e., what is the consistency of the EOS as presented in the Appendix. A very useful way of displaying all volume data is the following: Figure 13 shows schematically an isobar in the V-T plane. This isobar is characterized by three volumes: V_0 at $T=0$ K, V_{ms} in the solid, and V_{mf} in the liquid at the melting line. Plotting now three sets of volume data $\Delta V/V$, $(V_0-V_{\rm ref})/V_{\rm ref}$, $(V_{ms}-V_{\rm ref})/V_{\rm ref}$, and $(V_{mf}-V_{\rm ref})/V_{\rm ref}$ as a function of $V_{\rm ref}$ (our $T=0$ K isotherm), one can very easily compare all volume data from the literature with our EOS. In these plots (Figs. 14 and 15) the horizontal line at $\Delta V/V=0$ represents our $T=0$ K isotherm.

In Fig. 14 one finds all the data for the $T=0$ K isotherm. The points lie within 1–2 % around the reference line, our $T=0$ K isotherm. At the largest molar volume, the data point of Hoffer *et al.*[14] at $V=20.973$ cm^3/mole,

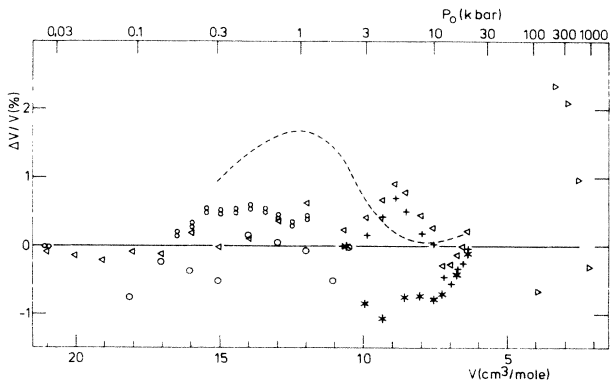

FIG. 14. Relative deviation in molar volume from our $T=0$ K isotherm. The following data are plotted: ○, Dugdale and Simon (Ref. 15); 8, Dugdale and Franck (Ref. 29); ✱, Stewart (Ref. 25); +, Stewart (Ref. 26); ∞, Hoffer *et al.* (Ref. 14); ◁, Swenson (Ref. 39); ▷, Young *et al.* (Ref. 37); dashed line, Spain and Segall (Ref. 3); solid line, our $T=0$ K isotherm.

$P=25.32$ bars is in excellent agreement with our EOS. The data of Dugdale and Simon[15] and Dugdale and Franck[29] are in reasonable agreement within their experimental uncertainty.

At higher pressure we see the two isotherms of Stewart,[25,26] which show a maximum deviation of 1.5% with respect to each other. But at high density, above 7 cm^3/mole, they give the same value. Our isotherm follows a kind of average of both. In this way all but one point of the Stewart isotherm lie within 0.8% of our isotherm. Spain and Segall[3] (dashed line) used the smoothed function of Stewart[26] as their isotherm at $T=0$ K. This smoothed function differs up to 0.9% from the experimental data of Stewart and is extrapolated below 2 kbar. Using their smoothed function with the estimated reference volume of Stewart, 10.72 cm^3/mole at 2 kbar, instead of our value of 10.694 cm^3/mole, the large difference of up to 1.4% in volume can be explained.

Swenson[39] gives a set of volume data based on the literature before 1977. His points are in good agreement with our EOS. Swenson pointed out that there are small but systematic inconsistencies between the low- and high-pressure data leading, e.g., to an abrupt change in the bulk modulus of 10%. His conclusion is that the absolute accuracy for the molar volume above 20 kbar is not better than 0.1 cm^3/mole. In fact, all volume determinations in the literature below 20 kbar are in agreement with our EOS within this error of 0.1 cm^3/mole (with the exception of the data of Spain and Segall[3]). At very high density we have also plotted the calculated $T=0$ K points of Young *et al.*[37] Our EOS was fitted to these points, and the scatter is reasonable and surely less than the accuracy of the calculation.

In Fig. 15 the volume data along the melting line are plotted in the same way as in Fig. 14. The figure shows two groups of points: Between 1% and 4% above the $T=0$ K reference line, one finds the V_{ms} data (open symbols), and at about 6% the V_{mf} data (solid symbols). Our EOS in both cases is represented as a solid line. The V_{ms} curve shows a small change in slope at $V=10.5$ cm^3/mole because of the change from the low- to the high-pressure $T=0$ K isotherm. The data of Grilly[13] at low density are in good agreement. The points of Grilly and Mills[28] show a small systematic deviation, but agree within 0.6% with our EOS. The volume data of Spain and Segall[3] exhibit the same behavior as in the $T=0$ K plot, Fig. 14, but the difference between V_{ms} and V_0 is nearly the same as in our EOS. The data points of Mills *et al.*[36] at high densities, about 7 cm^3/mole, are systematically higher, but are within the experimental error bars. In order to give an idea of the accuracy of the calculation of Young *et al.*,[37] we plot their results from V_{ms} from 8 to 4 cm^3/mole. There is a large scatter clearly above the experimental accuracy in the overlap region with experiment, but the calculation remains within 3% of the experimental data.

At V_{mf} (solid symbols) one again finds our EOS as a full line. The data points from the literature for V_{mf} are in general the most reliable ones, as in the liquid there is easy control of having a homogenous sample without pressure gradients. The data points of Grilly and Mills[28] and Grilly[13] are in good agreement at low density above 11 cm^3/mole. For the sake of completeness, we also give points from them in the liquid along the bcc phase, which show a sharp discontinuity in the slope at a volume of 20.6 cm^3/mole. At about 10 cm^3/mole the data of Grilly and Mills[28] show a deviation of about 0.6% from our EOS. At this density there is a competition between their data and those of Stewart[25,26] at $T=0$ K. Our EOS gives an average, whereas Spain and Segall[3] follow closely the data of Grilly and Mills[28] for V_{mf}.

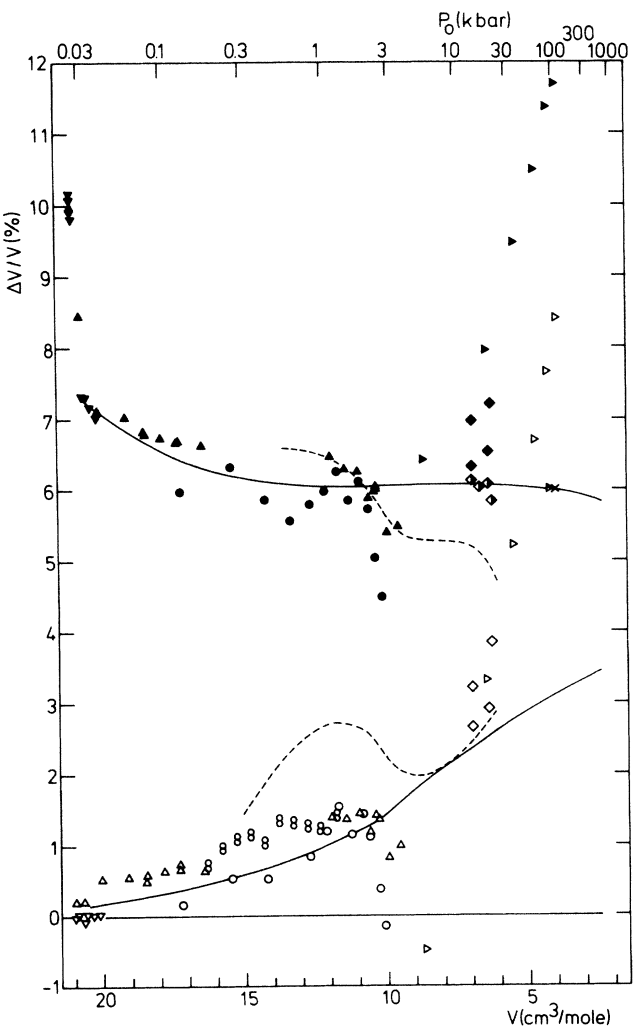

FIG. 15. Relative deviation in molar volume from our $T=0$ K isotherm. The following V_{ms} (open symbols) and V_{mf} (closed symbols) are plotted: ○,●, Dugdale and Simon (Ref. 15); 8: Dugdale and Franck (Ref. 29); △,▲, Grilly and Mills (Ref. 28); ▽,▼, Grilly (Ref. 13); ◇,◆, Mills *et al.* (Ref. 36) (◆, V_{mf} relative to our V_{ms}); ▷,▶; Young *et al.* (Ref. 37) (◗; V_{mf} relative to our V_{ms}); ×, V_{mf} data relative to our V_{ms} by Loubeyre *et al.* (Ref. 1). Dashed lines, Spain and Segall (Ref. 3); solid lines, our EOS.

TABLE VI. Equation of state of ^{4}He (low densities). The values are given in the following units: volume V, cm^3/mole; T and Θ_D, K; T/T_{ms} and γ, dimensionless; A, 10^{-6} K^{-1}; P and B, bar (low density, $V \geq 10.5$ cm^3/mole). (See Appendix for further details.)

T/T_{ms}	0.0	0.4	0.6	0.7	0.8	0.9	1	Fluid
			$V=21.00$	$\Theta_D=22.62$	$\gamma=2.572$			
T	0.00	0.66	0.98	1.15	1.31	1.47	1.64	2.26
P	25.198	25.207	25.246	25.287	25.349	25.441	25.568	47.835
B	269.59	269.47	269.20	268.91	268.47	267.84	266.95	
A	0.0	219.7	732.5	1161.2	1732.9	2469.0	3390.6	
			$V=20.75$	$\Theta_D=23.33$	$\gamma=2.563$			
T	0.00	0.70	1.05	1.22	1.39	1.57	1.74	2.38
P	28.554	28.565	28.610	28.658	28.732	28.839	28.989	52.668
B	291.03	290.83	290.51	290.18	289.67	288.92	287.89	
A	0.0	224.6	750.2	1189.7	1776.0	2530.7	3475.2	
			$V=20.50$	$\Theta_D=24.06$	$\gamma=2.554$			
T	0.00	0.74	1.11	1.30	1.48	1.67	1.85	2.51
P	32.220	32.233	32.286	32.342	32.429	32.555	32.730	57.932
B	314.13	314.05	313.67	313.28	312.69	311.81	310.61	
A	0.0	228.9	765.7	1214.7	1813.7	2584.7	3548.8	
			$V=20.25$	$\Theta_D=24.83$	$\gamma=2.545$			
T	0.00	0.79	1.18	1.38	1.57	1.77	1.97	2.64
P	36.225	36.241	36.303	36.369	36.470	36.616	36.821	63.639
B	339.05	338.72	338.29	337.83	337.14	336.12	334.72	
A	0.0	232.9	779.8	1237.6	1848.2	2634.1	3615.8	
			$V=20.00$	$\Theta_D=25.62$	$\gamma=2.536$			
T	0.00	0.84	1.25	1.46	1.67	1.88	2.09	2.79
P	40.603	40.620	40.693	40.770	40.888	41.060	41.299	69.827
B	365.95	366.03	365.53	365.00	364.18	363.01	361.38	
A	0.0	236.8	793.9	1260.3	1882.5	2682.8	3681.3	
			$V=19.75$	$\Theta_D=26.45$	$\gamma=2.527$			
T	0.00	0.89	1.33	1.55	1.77	2.00	2.22	2.94
P	45.387	45.407	45.492	45.582	45.720	45.920	46.198	76.611
B	395.02	395.03	394.45	393.83	392.89	391.52	389.64	
A	0.0	240.8	807.9	1282.8	1916.2	2730.6	3745.1	
			$V=19.50$	$\Theta_D=27.32$	$\gamma=2.518$			
T	0.00	0.94	1.41	1.65	1.88	2.12	2.35	3.10
P	50.617	50.641	50.739	50.843	51.003	51.236	51.558	83.977
B	426.46	426.37	425.69	424.98	423.89	422.32	420.15	
A	0.0	243.7	818.4	1299.8	1941.7	2766.3	3791.8	
			$V=19.25$	$\Theta_D=28.22$	$\gamma=2.509$			
T	0.00	1.00	1.50	1.75	2.00	2.25	2.50	3.27
P	56.337	56.365	56.479	56.600	56.786	57.056	57.431	91.978
B	460.51	460.06	459.28	458.46	457.19	455.37	452.88	
A	0.0	247.1	830.7	1319.6	1971.4	2807.6	3845.5	
			$V=19.00$	$\Theta_D=29.15$	$\gamma=2.500$			
T	0.00	1.06	1.59	1.85	2.12	2.38	2.65	3.44
P	62.59	62.63	62.76	62.90	63.11	63.43	63.86	100.72
B	497.40	497.25	496.35	495.40	493.95	491.86	489.01	
A	0.0	249.0	837.6	1330.7	1987.8	2829.8	3872.5	
			$V=18.75$	$\Theta_D=30.13$	$\gamma=2.490$			
T	0.00	1.13	1.69	1.97	2.25	2.53	2.81	3.63
P	69.45	69.48	69.64	69.80	70.05	70.41	70.91	110.27
B	537.44	536.91	535.87	534.78	533.11	530.69	527.42	
A	0.0	252.2	848.9	1348.8	2014.5	2866.3	3918.2	

TABLE VI. (*Continued*).

T/T_{ms}	0.0	0.4	0.6	0.7	0.8	0.9	1	Fluid
			$V=18.50$ $\Theta_D=31.16$ $\gamma=2.481$					
T	0.00	1.19	1.79	2.09	2.39	2.68	2.98	3.83
P	76.95	76.99	77.17	77.36	77.65	78.06	78.64	120.71
B	580.91	580.75	579.56	578.29	576.36	573.61	569.85	
A	0.0	254.0	855.3	1359.1	2029.5	2885.5	3939.8	
			$V=18.25$ $\Theta_D=32.22$ $\gamma=2.471$					
T	0.00	1.27	1.90	2.21	2.53	2.85	3.16	4.04
P	85.17	85.22	85.42	85.64	85.98	86.46	87.12	132.09
B	628.17	628.14	626.76	625.31	623.10	619.92	615.66	
A	0.0	255.5	861.0	1368.2	2042.4	2901.7	3956.2	
			$V=18.00$ $\Theta_D=33.34$ $\gamma=2.461$					
T	0.00	1.34	2.01	2.35	2.68	3.02	3.36	4.27
P	94.18	94.24	94.48	94.73	95.11	95.67	96.44	144.60
B	679.61	679.05	677.47	675.81	673.27	669.66	664.82	
A	0.0	256.8	865.9	1375.9	2053.2	2914.1	3967.1	
			$V=17.75$ $\Theta_D=34.50$ $\gamma=2.451$					
T	0.00	1.42	2.14	2.49	2.85	3.20	3.56	4.50
P	104.08	104.14	104.42	104.71	105.15	105.79	106.67	158.20
B	735.66	734.95	733.13	731.22	728.31	724.18	718.68	
A	0.0	258.1	870.7	1383.3	2063.0	2924.8	3974.7	
			$V=17.50$ $\Theta_D=35.72$ $\gamma=2.442$					
T	0.00	1.51	2.27	2.65	3.02	3.40	3.78	4.74
P	114.94	115.02	115.33	115.67	116.18	116.92	117.93	173.16
B	796.78	795.96	793.89	791.69	788.35	783.65	777.41	
A	0.0	259.3	874.8	1389.7	2071.2	2932.5	3977.4	
			$V=17.25$ $\Theta_D=37.00$ $\gamma=2.431$					
T	0.00	1.60	2.40	2.81	3.21	3.61	4.01	5.00
P	126.88	126.97	127.33	127.72	128.30	129.15	130.31	189.65
B	863.53	863.43	861.04	858.53	854.74	849.37	842.31	
A	0.0	259.2	874.8	1389.2	2068.8	2925.0	3959.1	
			$V=17.00$ $\Theta_D=38.33$ $\gamma=2.421$					
T	0.00	1.70	2.55	2.98	3.40	3.83	4.25	5.27
P	140.01	140.11	140.53	140.98	141.65	142.63	143.96	207.55
B	936.49	934.93	932.18	929.30	924.97	918.92	910.93	
A	0.0	259.9	877.4	1393.0	2072.5	2925.1	3950.4	
			$V=16.75$ $\Theta_D=39.73$ $\gamma=2.411$					
T	0.00	1.81	2.71	3.16	3.61	4.06	4.51	5.56
P	154.47	154.59	155.07	155.58	156.36	157.47	159.00	227.44
B	1016.3	1015.5	1012.3	1009.0	1004.1	997.2	988.3	
A	0.0	259.4	875.7	1389.6	2065.2	2909.6	3919.8	
			$V=16.50$ $\Theta_D=41.19$ $\gamma=2.401$					
T	0.00	1.91	2.87	3.35	3.82	4.30	4.78	5.87
P	170.40	170.54	171.09	171.67	172.55	173.82	175.55	249.24
B	1103.9	1103.0	1099.5	1095.7	1090.2	1082.4	1072.4	
A	0.0	257.1	868.1	1376.9	2043.9	2874.4	3863.0	
			$V=16.25$ $\Theta_D=42.73$ $\gamma=2.390$					
T	0.00	2.02	3.04	3.54	4.05	4.55	5.06	6.21
P	187.98	188.13	188.76	189.42	190.42	191.86	193.82	273.33
B	1199.9	1198.2	1194.2	1190.0	1183.7	1175.1	1163.9	
A	0.0	254.2	858.5	1361.0	2017.7	2832.2	3797.2	

TABLE VI. (*Continued*).

T/T_{ms}	0.0	0.4	0.6	0.7	0.8	0.9	1	Fluid
			$V=16.00$ $\Theta_D=44.34$ $\gamma=2.380$					
T	0.00	2.15	3.22	3.76	4.29	4.83	5.37	6.56
P	207.39	207.57	208.28	209.04	210.19	211.83	214.05	299.78
B	1305.3	1303.9	1299.3	1294.5	1287.4	1277.7	1265.2	
A	0.0	252.3	851.9	1349.4	1997.7	2797.8	3740.6	
			$V=15.75$ $\Theta_D=46.02$ $\gamma=2.369$					
T	0.00	2.28	3.41	3.98	4.55	5.12	5.69	6.94
P	228.85	229.05	229.86	230.73	232.03	233.90	236.41	329.05
B	1421.3	1419.7	1414.5	1409.1	1401.1	1390.2	1376.3	
A	0.0	249.3	841.6	1332.0	1968.8	2751.0	3667.6	
			$V=15.50$ $\Theta_D=47.80$ $\gamma=2.358$					
T	0.00	2.42	3.63	4.23	4.83	5.44	6.04	7.35
P	252.60	252.83	253.77	254.76	256.26	258.39	261.26	361.24
B	1549.1	1548.5	1542.5	1536.4	1527.3	1515.0	1499.5	
A	0.0	247.5	835.2	1320.5	1948.0	2714.6	3607.5	
			$V=15.25$ $\Theta_D=49.66$ $\gamma=2.348$					
T	0.00	2.56	3.85	4.49	5.13	5.77	6.41	7.79
P	278.92	279.18	280.25	281.38	283.10	285.52	288.77	397.15
B	1690.0	1688.1	1681.4	1674.4	1664.2	1650.4	1633.2	
A	0.0	244.5	825.0	1302.9	1918.3	2666.0	3531.7	
			$V=15.00$ $\Theta_D=51.62$ $\gamma=2.337$					
T	0.00	2.73	4.09	4.78	5.46	6.14	6.82	8.26
P	308.12	308.42	309.66	310.97	312.93	315.71	319.43	436.74
B	1845.6	1845.1	1837.3	1829.4	1817.7	1802.2	1782.9	
A	0.0	242.7	818.3	1290.7	1895.7	2626.4	3466.5	
			$V=14.75$ $\Theta_D=53.69$ $\gamma=2.325$					
T	0.00	2.90	4.35	5.08	5.80	6.53	7.25	8.77
P	340.56	340.92	342.34	343.83	346.09	349.26	353.48	480.96
B	2017.7	2014.8	2006.0	1996.9	1983.8	1966.5	1945.0	
A	0.0	240.2	809.5	1274.8	1867.9	2579.5	3392.3	
			$V=14.50$ $\Theta_D=55.86$ $\gamma=2.314$					
T	0.00	3.09	4.63	5.41	6.18	6.95	7.72	9.31
P	376.66	377.07	378.71	380.44	383.03	386.67	391.49	529.81
B	2208.3	2207.2	2197.0	2186.7	2171.9	2152.3	2128.4	
A	0.0	238.0	801.4	1259.8	1840.6	2532.7	3317.5	
			$V=14.25$ $\Theta_D=58.15$ $\gamma=2.303$					
T	0.00	3.29	4.94	5.76	6.58	7.41	8.23	9.90
P	416.88	417.35	419.25	421.24	424.22	428.39	433.90	584.43
B	2419.8	2419.2	2407.6	2395.7	2378.9	2357.0	2330.4	
A	0.0	235.7	792.8	1243.8	1811.6	2483.4	3239.6	
			$V=14.00$ $\Theta_D=60.56$ $\gamma=2.291$					
T	0.00	3.51	5.27	6.14	7.02	7.90	8.78	10.53
P	461.76	462.30	464.50	466.81	470.24	475.03	481.33	644.92
B	2654.7	2652.9	2639.5	2626.0	2607.0	2582.3	2552.7	
A	0.0	233.7	784.9	1228.5	1783.2	2434.7	3162.2	
			$V=13.75$ $\Theta_D=63.10$ $\gamma=2.280$					
T	0.00	3.75	5.62	6.55	7.49	8.43	9.36	11.21
P	511.91	512.54	515.09	517.76	521.72	527.21	534.40	712.63
B	2916.1	2911.9	2896.5	2881.2	2859.6	2831.9	2799.0	
A	0.0	231.4	776.2	1211.7	1752.6	2382.8	3080.9	

TABLE VI. (*Continued*).

T/T_{ms}	0.0	0.4	0.6	0.7	0.8	0.9	1	Fluid
			$V=13.50$ $\Theta_D=65.79$ $\gamma=2.268$					
T	0.00	4.00	6.00	7.00	8.00	9.00	10.00	11.94
P	568.05	568.79	571.76	574.85	579.43	585.76	594.00	788.50
B	3207.5	3205.2	3187.4	3169.7	3145.3	3114.3	3077.5	
A	0.0	229.3	767.7	1195.0	1721.7	2330.3	2999.1	
			$V=13.25$ $\Theta_D=68.63$ $\gamma=2.256$					
T	0.00	4.28	6.41	7.48	8.55	9.62	10.69	12.74
P	631.00	631.86	635.31	638.89	644.17	651.43	660.85	873.54
B	3532.8	3526.6	3506.2	3486.1	3458.4	3423.7	3383.1	
A	0.0	226.8	757.5	1175.6	1686.8	2272.4	2910.6	
			$V=13.00$ $\Theta_D=71.64$ $\gamma=2.244$					
T	0.00	4.58	6.86	8.01	9.15	10.30	11.44	13.60
P	701.71	702.71	706.74	710.91	717.03	725.40	736.20	968.93
B	3896.7	3891.4	3867.8	3844.8	3813.4	3774.5	3729.3	
A	0.0	224.6	748.1	1156.8	1652.2	2214.6	2822.0	
			$V=12.75$ $\Theta_D=74.82$ $\gamma=2.231$					
T	0.00	4.90	7.36	8.58	9.81	11.03	12.26	14.54
P	781.3	782.4	787.2	792.0	799.1	808.8	821.2	1076.0
B	4304.4	4298.1	4270.8	4244.3	4208.8	4165.1	4115.0	
A	0.0	222.7	739.4	1138.8	1618.3	2157.5	2734.5	
			$V=12.50$ $\Theta_D=78.19$ $\gamma=2.219$					
T	0.00	5.26	7.89	9.20	10.52	11.83	13.15	15.56
P	871.0	872.3	877.9	883.6	891.8	903.0	917.2	1197.1
B	4762.1	4755.2	4723.5	4693.3	4652.9	4604.0	4548.6	
A	0.0	220.6	729.6	1118.8	1581.5	2096.6	2642.7	
			$V=12.25$ $\Theta_D=81.76$ $\gamma=2.206$					
T	0.00	5.64	8.46	9.87	11.28	12.69	14.10	16.66
P	972.3	973.9	980.4	987.0	996.6	1009.5	1025.8	1333.2
B	5277.0	5267.8	5231.0	5196.3	5150.8	5096.1	5034.8	
A	0.0	218.1	718.1	1096.0	1540.8	2031.0	2545.8	
			$V=12.00$ $\Theta_D=85.56$ $\gamma=2.193$					
T	0.00	6.07	9.10	10.62	12.13	13.65	15.17	17.86
P	1087.0	1088.9	1096.6	1104.4	1115.6	1130.5	1149.3	1487.1
B	5857.3	5847.7	5804.6	5765.0	5713.3	5652.1	5584.3	
A	0.0	216.4	708.9	1076.1	1503.6	1969.6	2454.0	
			$V=11.75$ $\Theta_D=89.59$ $\gamma=2.180$					
T	0.00	6.53	9.79	11.42	13.05	14.68	16.32	19.18
P	1217.1	1219.4	1228.4	1237.5	1250.6	1267.9	1289.6	1662.3
B	6512.8	6499.8	6449.7	6404.3	6345.9	6277.6	6202.6	
A	0.0	214.2	697.4	1052.8	1461.8	1902.7	2356.5	
			$V=11.50$ $\Theta_D=93.88$ $\gamma=2.167$					
T	0.00	7.03	10.54	12.30	14.06	15.82	17.57	20.61
P	1365.0	1367.7	1378.4	1389.1	1404.3	1424.4	1449.4	1860.3
B	7254.8	7237.6	7179.4	7127.3	7061.3	6985.1	6902.5	
A	0.0	212.0	685.5	1028.6	1418.8	1834.7	2258.2	
			$V=11.25$ $\Theta_D=98.44$ $\gamma=2.154$					
T	0.00	7.59	11.38	13.28	15.17	17.07	18.97	22.18
P	1533.5	1536.8	1549.5	1562.1	1580.0	1603.3	1632.2	2086.3
B	8096.6	8076.3	8008.2	7948.3	7873.6	7788.5	7697.4	
A	0.0	210.3	674.5	1005.2	1376.6	1767.8	2161.9	

TABLE VI. (*Continued*).

T/T_{ms}	0.0	0.4	0.6	0.7	0.8	0.9	1	Fluid
			$V=11.00$ $\Theta_D=103.31$ $\gamma=2.140$					
T	0.00	8.19	12.28	14.33	16.37	18.42	20.47	23.89
P	1726.0	1729.9	1745.0	1759.9	1780.7	1807.8	1841.1	2343.8
B	9054.0	9033.1	8953.7	8885.1	8800.9	8706.4	8606.4	
A	0.0	207.6	660.1	977.1	1328.4	1694.1	2058.6	
			$V=10.75$ $\Theta_D=108.50$ $\gamma=2.127$					
T	0.00	8.85	13.28	15.49	17.71	19.92	22.13	25.78
P	1946.5	1951.1	1969.2	1986.7	2011.2	2042.7	2081.1	2639.1
B	10146.0	10122.0	10029.0	9950.0	9856.0	9750.0	9640.0	
A	0.0	205.4	646.5	949.6	1281.2	1622.1	1958.1	
			$V=10.50$ $\Theta_D=114.05$ $\gamma=2.113$					
T	0.00	9.60	14.40	16.79	19.19	21.59	23.99	27.85
P	2199.6	2205.2	2226.9	2247.7	2276.5	2313.3	2357.9	2976.1
B	11393.0	11362.0	11253.0	11164.0	11057.0	10940.0	10819.0	
A	0.0	203.7	633.7	923.2	1235.3	1552.0	1860.6	

TABLE VII. Equation of state of ^{4}He (high densities). The values are given in the following units: volume V, cm^3/mole; T and Θ_D, K; T/T_{ms} and γ, dimensionless; A, 10^{-6} K^{-1}; P and B, kbar (high density, $V<10.5$ cm^3/mole). (See Appendix for further details.)

T/T_{ms}	0.0	0.4	0.6	0.7	0.8	0.9	1	Fluid
			$V=10.50$ $\Theta_D=114.05$ $\gamma=2.113$					
T	0.00	9.60	14.40	16.80	19.20	21.59	23.99	27.88
P	2.1982	2.2038	2.2254	2.2463	2.2750	2.3119	2.3565	2.9818
B	11.809	11.778	11.670	11.579	11.473	11.355	11.235	
A	0.0	196.5	611.2	890.2	1190.6	1495.3	1791.9	
			$V=10.25$ $\Theta_D=119.99$ $\gamma=2.099$					
T	0.00	10.42	15.64	18.24	20.85	23.46	26.06	30.09
P	2.4968	2.5036	2.5296	2.5545	2.5885	2.6316	2.6834	3.3577
B	12.989	12.952	12.824	12.720	12.600	12.470	12.338	
A	0.0	199.7	613.0	884.9	1173.6	1462.5	1740.5	
			$V=10.00$ $\Theta_D=126.35$ $\gamma=2.084$					
T	0.00	11.33	16.99	19.83	22.66	25.49	28.32	32.47
P	2.8336	2.8418	2.8732	2.9028	2.9428	2.9932	3.0534	3.7808
B	14.312	14.267	14.117	13.999	13.863	13.720	13.576	
A	0.0	202.3	612.3	876.0	1151.8	1424.3	1683.6	
			$V=9.75$ $\Theta_D=133.17$ $\gamma=2.070$					
T	0.00	12.30	18.45	21.53	24.60	27.68	30.75	35.04
P	3.2144	3.2244	3.2619	3.2968	3.3437	3.4023	3.4718	4.2580
B	15.797	15.755	15.580	15.446	15.294	15.136	14.980	
A	0.0	203.4	606.6	860.3	1121.9	1377.3	1617.8	
			$V=9.50$ $\Theta_D=140.50$ $\gamma=2.055$					
T	0.00	13.35	20.02	23.36	26.70	30.04	33.37	37.85
P	3.6462	3.6581	3.7028	3.7438	3.7985	3.8664	3.9463	4.8010
B	17.469	17.406	17.203	17.052	16.882	16.709	16.540	
A	0.0	203.5	597.9	840.7	1087.9	1326.4	1548.6	
			$V=9.25$ $\Theta_D=148.38$ $\gamma=2.040$					
T	0.00	14.50	21.75	25.38	29.01	32.63	36.26	40.90
P	4.1368	4.1512	4.2044	4.2527	4.3165	4.3950	4.4871	5.4167
B	19.357	19.285	19.050	18.879	18.692	18.502	18.320	
A	0.0	203.0	587.2	818.4	1050.7	1272.2	1476.5	

TABLE VII. (*Continued*).

T/T_{ms}	0.0	0.4	0.6	0.7	0.8	0.9	1	Fluid
			$V=9.00$ $\Theta_D=156.87$ $\gamma=2.024$					
T	0.00	15.75	23.63	27.57	31.51	35.45	39.38	44.22
P	4.6960	4.7133	4.7763	4.8329	4.9070	4.9977	5.1033	6.1167
B	21.495	21.412	21.142	20.950	20.742	20.535	20.339	
A	0.0	201.4	573.1	792.1	1009.1	1213.9	1401.0	
			$V=8.75$ $\Theta_D=166.04$ $\gamma=2.009$					
T	0.00	17.12	25.68	29.96	34.24	38.52	42.80	47.84
P	5.3352	5.3559	5.4305	5.4966	5.5827	5.6872	5.8083	6.9148
B	23.924	23.820	23.510	23.294	23.065	22.840	22.629	
A	0.0	199.0	557.0	763.3	965.3	1153.7	1324.4	
			$V=8.50$ $\Theta_D=175.96$ $\gamma=1.993$					
T	0.00	18.62	27.93	32.59	37.24	41.90	46.55	51.83
P	6.0681	6.0929	6.1812	6.2585	6.3583	6.4787	6.6175	7.8328
B	26.692	26.550	26.194	25.953	25.701	25.456	25.231	
A	0.0	196.0	539.4	733.0	920.2	1093.0	1248.1	
			$V=8.25$ $\Theta_D=186.70$ $\gamma=1.976$					
T	0.00	20.26	30.38	35.45	40.51	45.58	50.64	56.21
P	6.9113	6.9409	7.0451	7.1352	7.2507	7.3891	7.5479	8.8862
B	29.857	29.713	29.306	29.037	28.761	28.495	28.253	
A	0.0	191.7	518.6	699.0	871.4	1028.9	1169.2	
			$V=8.00$ $\Theta_D=198.35$ $\gamma=1.960$					
T	0.00	22.06	33.10	38.61	44.13	49.64	55.16	61.03
P	7.885	7.920	8.043	8.148	8.282	8.442	8.624	10.099
B	33.490	33.311	32.847	32.547	32.243	31.955	31.697	
A	0.0	187.2	497.5	665.0	823.2	966.4	1092.7	
			$V=7.75$ $\Theta_D=211.03$ $\gamma=1.943$					
T	0.00	24.06	36.10	42.11	48.13	54.15	60.16	66.34
P	9.013	9.056	9.201	9.324	9.479	9.663	9.871	11.501
B	37.677	37.483	36.953	36.619	36.286	35.974	35.699	
A	0.0	182.0	475.0	629.8	774.2	903.6	1016.8	
			$V=7.50$ $\Theta_D=224.85$ $\gamma=1.926$					
T	0.00	26.28	39.42	45.99	52.55	59.12	65.69	72.23
P	10.327	10.378	10.549	10.693	10.872	11.084	11.323	13.128
B	42.522	42.281	41.676	41.305	40.940	40.605	40.311	
A	0.0	176.40	451.86	594.28	725.54	842.03	943.14	
			$V=7.25$ $\Theta_D=239.95$ $\gamma=1.908$					
T	0.00	28.74	43.11	50.29	57.48	64.66	71.85	78.83
P	11.862	11.923	12.126	12.294	12.502	12.747	13.021	15.040
B	48.154	47.872	47.182	46.770	46.371	46.008	45.697	
A	0.00	170.33	428.02	558.33	677.07	781.42	871.20	
			$V=7.00$ $\Theta_D=256.48$ $\gamma=1.890$					
T	0.00	31.51	47.26	55.14	63.02	70.90	78.77	86.12
P	13.665	13.739	13.980	14.176	14.419	14.702	15.019	17.259
B	54.734	54.394	53.606	53.148	52.711	52.321	51.991	
A	0.00	164.21	404.37	523.08	629.95	722.93	802.33	
			$V=6.75$ $\Theta_D=274.65$ $\gamma=1.872$					
T	0.00	34.63	51.94	60.60	69.25	77.91	86.57	94.34
P	15.793	15.883	16.170	16.401	16.685	17.013	17.379	19.890
B	62.458	62.049	61.149	60.640	60.162	59.744	59.395	
A	0.00	157.88	380.63	488.19	583.84	666.28	736.04	

TABLE VII. (*Continued.*)

T/T_{ms}	0.0	0.4	0.6	0.7	0.8	0.9	1	Fluid
			$V=6.50$ $\Theta_D=294.65$ $\gamma=1.853$					
T	0.00	38.09	57.13	66.66	76.18	85.70	95.22	104.10
P	18.318	18.427	18.770	19.041	19.372	19.753	20.177	23.026
B	71.579	71.085	70.059	69.493	68.972	68.523	68.155	
A	0.00	150.79	356.02	452.86	538.00	610.73	671.73	
			$V=6.25$ $\Theta_D=316.75$ $\gamma=1.834$					
T	0.00	42.28	63.43	74.00	84.57	95.14	105.71	114.93
P	21.333	21.469	21.887	22.212	22.605	23.055	23.552	26.755
B	82.411	81.810	80.626	79.996	79.429	78.949	78.567	
A	0.00	145.86	335.16	421.91	497.10	560.58	613.34	
			$V=6.00$ $\Theta_D=341.24$ $\gamma=1.815$					
T	0.00	46.94	70.41	82.14	93.88	105.61	117.35	127.17
P	24.956	25.124	25.631	26.018	26.484	27.014	27.596	31.216
B	95.362	94.646	93.285	92.585	91.968	91.458	91.063	
A	0.00	139.52	312.41	389.53	455.48	510.50	555.87	
			$V=5.75$ $\Theta_D=368.48$ $\gamma=1.795$					
T	0.00	52.25	78.37	91.44	104.50	117.56	130.62	141.08
P	29.338	29.548	30.164	30.628	31.181	31.807	32.492	36.585
B	110.95	110.12	108.55	107.78	107.11	106.57	106.16	
A	0.00	132.74	289.45	357.42	414.79	462.24	500.97	
			$V=5.50$ $\Theta_D=398.91$ $\gamma=1.774$					
T	0.00	58.33	87.49	102.07	116.66	131.24	145.82	157.16
P	34.680	34.943	35.694	36.251	36.911	37.653	38.461	43.177
B	129.87	128.87	127.08	126.22	125.49	124.93	124.52	
A	0.00	125.59	266.46	325.90	375.39	415.86	448.73	
			$V=5.25$ $\Theta_D=433.02$ $\gamma=1.753$					
T	0.00	65.33	98.00	114.33	130.66	146.99	163.33	175.63
P	41.245	41.576	42.496	43.168	43.958	44.841	45.798	51.231
B	153.01	151.71	149.65	148.69	147.92	147.33	146.92	
A	0.00	118.19	243.82	295.33	337.75	371.99	399.56	
			$V=5.00$ $\Theta_D=471.45$ $\gamma=1.732$					
T	0.00	73.56	110.35	128.74	147.13	165.52	183.91	196.98
P	49.389	49.810	50.947	51.764	52.717	53.775	54.917	61.151
B	181.59	180.10	177.72	176.67	175.84	175.24	174.85	
A	0.00	110.76	221.70	265.79	301.60	330.20	353.12	
			$V=4.75$ $\Theta_D=514.95$ $\gamma=1.710$					
T	0.00	83.11	124.66	145.44	166.21	186.99	207.77	222.19
P	59.590	60.128	61.539	62.535	63.689	64.962	66.331	73.668
B	217.23	215.41	212.67	211.52	210.64	210.03	209.67	
A	0.00	102.92	199.78	237.17	267.10	290.82	309.64	
			$V=4.50$ $\Theta_D=564.48$ $\gamma=1.687$					
T	0.00	94.34	141.51	165.10	188.68	212.27	235.86	251.71
P	72.513	73.207	74.968	76.191	77.596	79.140	80.791	89.382
B	262.19	259.79	256.64	255.38	254.46	253.86	253.55	
A	0.00	94.96	178.56	209.82	234.60	253.92	269.19	
			$V=4.25$ $\Theta_D=621.20$ $\gamma=1.664$					
T	0.00	107.89	161.83	188.80	215.77	242.74	269.71	287.29
P	89.09	90.00	92.22	93.74	95.47	97.36	99.37	109.74
B	319.61	316.80	313.18	311.82	310.87	310.30	310.08	
A	0.00	87.06	158.08	183.82	203.84	219.45	231.59	

TABLE VII. (*Continued.*)

T/T_{ms}	0.0	0.4	0.6	0.7	0.8	0.9	1	Fluid
			$V=4.00$	$\Theta_D=686.63$	$\gamma=1.640$			
T	0.00	124.05	186.07	217.08	248.09	279.10	310.12	329.62
P	110.64	111.84	114.68	116.57	118.72	121.05	123.52	135.88
B	393.98	390.22	386.05	384.59	383.63	383.14	383.06	
A	0.00	78.99	138.39	159.19	175.19	187.51	197.14	
			$V=3.75$	$\Theta_D=762.67$	$\gamma=1.615$			
T	0.00	143.90	215.85	251.82	287.80	323.77	359.75	381.43
P	139.11	140.72	144.39	146.79	149.49	152.40	155.48	170.54
B	491.83	487.30	482.51	480.98	480.07	479.72	479.85	
A	0.00	70.94	119.51	135.89	148.41	157.95	165.36	
			$V=3.50$	$\Theta_D=851.81$	$\gamma=1.590$			
T	0.00	168.22	252.33	294.38	336.43	378.49	420.54	445.58
P	177.39	179.59	184.38	187.45	190.88	194.56	198.42	217.27
B	622.92	617.08	611.62	610.03	609.25	609.12	609.57	
A	0.00	62.74	101.44	114.08	123.62	130.87	136.53	
			$V=3.25$	$\Theta_D=957.37$	$\gamma=1.563$			
T	0.00	198.84	298.27	347.98	397.69	447.40	497.11	525.35
P	229.92	232.98	239.35	243.35	247.77	252.49	257.42	280.88
B	802.16	794.47	788.29	786.76	786.21	786.46	787.41	
A	0.00	54.58	84.36	93.76	100.82	106.14	110.31	
			$V=3.00$	$\Theta_D=1083.80$	$\gamma=1.536$			
T	0.00	237.78	356.67	416.12	475.57	535.01	594.46	627.26
P	303.72	308.09	316.69	321.97	327.78	333.93	340.34	370.39
B	1053.1	1043.1	1036.2	1034.9	1034.8	1035.6	1037.3	
A	0.000	46.317	68.194	74.888	79.908	83.679	86.761	
			$V=2.75$	$\Theta_D=1237.29$	$\gamma=1.508$			
T	0.00	288.57	432.86	505.00	577.14	649.29	721.43	759.42
P	410.31	416.70	428.60	435.73	443.51	451.70	460.20	499.22
B	1414.5	1401.3	1393.9	1393.0	1393.7	1395.6	1398.4	
A	0.000	38.003	53.036	57.507	60.919	63.650	65.797	
			$V=2.50$	$\Theta_D=1426.61$	$\gamma=1.480$			
T	0.00	356.29	534.44	623.51	712.58	801.65	890.73	935.19
P	569.39	579.05	595.91	605.79	616.47	627.65	639.18	691.07
B	1952.2	1934.4	1926.9	1927.0	1929.0	1932.5	1937.3	
A	0.000	29.591	38.832	41.648	43.903	45.783	47.345	

The points of Mills *et al.*[36] at high densities show the same behavior as for V_{ms}; this is also true for those of Young *et al.*[37] In order to show the consistency of the V_{ms} and V_{mf} data, we also plot V_{mf} data with respect to V_{ms} from our EOS, i.e., we use the volume change on melting. In this way the points of Mills *et al.*,[36] Young *et al.*,[37] and Loubeyre *et al.*[1] closely follow our EOS (which is based on these data), and show their consistency in the determination of $V_{mf}-V_{ms}$.

The main problem in the EOS at highest densities below 6 cm^3/mole is that there are no experimental static volume determinations. The calculations of Young *et al.*[37] show reasonable agreement in the overlap region, within 3%, and give the correct ΔV upon melting at 150 kbar. There is a comparison with shock-wave experiments (see Fig. 11) taken from Ref. 2 which are done at very high temperature in the liquid. Young *et al.* pointed out that because of the high temperature the shock-wave measurements give a good check for the potential at small interatomic distances. The fairly good agreement between shock wave and calculation for the single-shock data (within 3%) at pressures up to 150 kbar and $T\approx 10\,000$

K, together with the reasonable agreement with the static low-pressure experimental data below 20 kbar, give support to the potential used in the short- and medium-long-distance range.

As can be seen from Fig. 15, there is a disagreement of about 5.5% between the calculation of Young *et al.* and our EOS at the molar volume 4 cm^3/mole (150 kbar). Together with the uncertainty in the shock-wave data at the same pressure (3%), the total error is not expected to exceed 7% at these densities. At pressures above 150 kbar, where there is only one double-shock point at 558 kbar, the volume determination is less accurate, and the LMTO calculation shows a deviation outside the experimental accuracy (see Fig. 11). The extrapolation above 150 kbar therefore should be seen as a crude indication of the high-pressure behavior. A careful analysis of the shock-wave data, and especially static experiments in the diamond-anvil cell, are desirable, to give a reliable EOS at the highest densities.

ACKNOWLEDGMENTS

This research was supported by the Dutch Foundation Stichting voor Fundamenteel Onderzoek der Materie, and by the National Science Foundation, Low Temperature Physics Program, under Grant No. DMR-82-13662.

APPENDIX

In Tables VI and VII we present the EOS for helium at low and medium densities from 21 to 6 cm^3/mole and an extrapolation from 6 to 2.5 cm^3/mole. We give for a dense set of volumes the pressure P, the bulk modulus $B=-V\partial P/\partial V$ and the thermal expansion $A=-(1/V)(\partial V/\partial T)$ along an isochore as a function of the reduced temperature T/T_{ms}, where T_{ms} is the melting temperature.

For the calculation of the thermal properties we use a temperature-independent Debye temperature Θ_D and Grüneisen parameter γ, which is given for each isochore. Although the accuracy of the listed values for the calculated thermodynamical variables exceeds the experimental limits, sometimes by 2—3 orders in magnitude, we believe that our presentation can be useful for interpolation and numerical calculation of other thermodynamical variables.

*Present address: Natuurkundig Laboratorium, Vrije Universiteit, Amsterdam, The Netherlands.

[1]P. Loubeyre, J. M. Besson, J. P. Pinceaux, and J. P. Hansen, Phys. Rev. Lett. **49**, 1172 (1982).
[2]W. J. Nellis, N. C. Holmes, A. C. Mitchell, R. J. Trainor, G. K. Governo, M. Ross, and D. A. Young, Phys. Rev. Lett. **53**, 1248 (1984).
[3]I. L. Spain and S. Segall, Cryogenics **11**, 26 (1971).
[4]A. Driessen and I. F. Silvera, J. Low Temp. Phys. **54**, 361 (1984); P. J. Berkhout and I. F. Silvera, *ibid.* **36**, 231 (1979).
[5](a) A. Driessen and I. F. Silvera, J. Low Temp. Phys. **54**, 565 (1984); (b) A. Driessen, Ph.D. thesis, University of Amsterdam, 1982 (unpublished).
[6]D. Lévesque, J. J. Weis, and M. L. Klein, Phys. Rev. Lett. **51**, 670 (1983).
[7]J. H. Vignos and H. A. Fairbank, Phys. Rev. Lett. **6**, 265 (1961).
[8]E. R. Grilly and R. L. Mills, Ann. Phys. (N.Y.) **18**, 250 (1962).
[9]G. Ahlers, Phys. Rev. **135**, A10 (1964).
[10]D. O. Edwards and R. C. Pandorf, Phys. Rev. **144**, 143 (1966).
[11]J. E. Vos, B. S. Blaisse, D. A. E. Boon, W. J. van Scherpenzeel, and R. Kingma, Physica **37**, 51 (1967).
[12]J. F. Jarvis, D. Ramm, and H. Meyer, Phys. Rev. **170**, 320 (1968).
[13]E. R. Grilly, J. Low Temp. Phys. **11**, 33 (1973).
[14]J. K. Hoffer, W. R. Gardner, C. G. Waterfield, and N. E. Phillips, J. Low Temp. Phys. **23**, 63 (1976).
[15]J. S. Dugdale and F. E. Simon, Proc. R. Soc. London, Ser. A **218**, 291 (1953).
[16]R. L. Mills and A. F. Schuch, Phys. Rev. Lett. **6**, 263 (1961).
[17]R. L. Mills and A. F. Schuch, J. Low. Temp. Phys. **16**, 305 (1974).
[18]J. P. Franck, Phys. Rev. Lett. **40**, 1272 (1978).
[19]J. P. Franck and W. B. Daniels, Phys. Rev. Lett. **44**, 259 (1980).
[20]J. P. Franck, Phys. Rev. B **22**, 4315 (1980).
[21]J. P. Franck, J. Low. Temp. Phys. **45**, 91 (1981).
[22]J. P. Franck and W. B. Daniels, Phys. Rev. B **24**, 2456 (1981).
[23]B. L. Holian, W. D. Gwinn, A. C. Luntz, and B. J. Alder, J. Chem. Phys. **59**, 5444 (1973).
[24]D. A. Young and B. J. Alder, J. Chem. Phys. **73**, 2430 (1980).
[25]J. W. Stewart, J. Phys. Chem. Solids **1**, 146 (1956).
[26]J. W. Stewart, Phys. Rev. **129**, 1950 (1963).
[27]R. L. Mills and E. R. Grilly, Phys. Rev. **99**, 480 (1955).
[28]E. R. Grilly and R. L. Mills, Ann. Phys. (N.Y.) **8**, 1 (1959).
[29]J. S. Dugdale and J. P. Franck, Philos. Trans. R. Soc. London **257**, 1 (1964).
[30]G. Ahlers, Phys. Lett. **24A**, 152 (1967).
[31]G. Ahlers, Phys. Rev. A **2**, 1505 (1970).
[32]D. O. Edwards and R. C. Pandorf, Phys. Rev. **140** A816 (1965).
[33]A. P. M. Glassford and J. L. Smith, Jr., Cryogenics **6**, 193 (1966).
[34]D. S. Betts, Cryogenics **16**, 3 (1976).
[35]J. K. Krause and C. A. Swenson, Cryogenics **16**, 413 (1976).
[36]R. L. Mills, D. H. Liebenberg, and J. C. Bronson, Phys. Rev. B **21**, 5137 (1980).
[37]D. A. Young, A. K. McMahan, and M. Ross, Phys. Rev. B **24**, 5119 (1981).
[38]J. Maynard, Phys. Rev. B **14**, 3868 (1976); J. Landau and G. G. Ihas, J. Low Temp. Phys. **29**, 445 (1977).
[39]C. A. Swenson, in *Rare Gas Solids,* edited by M. L. Klein and J. A. Venables (Academic, London, 1976), Vol. II, p. 823.
[40]A. Driessen, J. A. de Waal, and I. F. Silvera, J. Low Temp. Phys. **34**, 255 (1979).
[41]F. J. Edeskuty and R. H. Sherman, in *Proceedings of the 5th International Conference on Low Temperature Physics, Madison, Wisconsin, 1958,* edited by J. R. Dillinger (University of Wisconsin Press, Madison, 1958), p. 102.
[42]W. H. Keesom and A. P. Keesom, Physica **1**, 128 (1934).
[43]J. S. Dugdale, Nuovo Cimento Suppl. **9**, 27 (1958).
[44]F. R. Simon, M. Ruhemann, and W. A. M. Edwards, Z. Phys. Chem. **6**, 62 (1929).
[45]C. A. Swensen, Phys. Rev. **89**, 538 (1953).
[46]R. K. Crawford and W. B. Daniels, J. Chem. Phys. **55**, 5651 (1971).